

# A Toolbox for Quantifying Memory in Dynamics Along Reaction Coordinates

Alessio Lapolla and Aljaž Godec\*

*Mathematical bioPhysics Group, Max Planck Institute for Biophysical Chemistry, Göttingen 37077, Germany*

(Dated: October 17, 2021)

Memory effects in time-series of experimental observables are ubiquitous, have important consequences for the interpretation of kinetic data, and may even affect the function of biomolecular nanomachines such as enzymes. Here we propose a set of complementary methods for quantifying conclusively the magnitude and duration of memory in a time series of a reaction coordinate. The toolbox is general, robust, easy to use, and does not rely on any underlying microscopic model. As a proof of concept we apply it to the analysis of memory in the dynamics of the end-to-end distance of the analytically solvable Rouse-polymer model and an experimental time-series of extensions of a single DNA hairpin measured in an optical tweezers experiment.

The dynamics of complex, high-dimensional physical systems such as complex biomolecules is frequently described by means of memory-less, Markovian diffusion along a low-dimensional reaction coordinate [1–9]. Such simplified models often accurately describe selected observations in experiments [10–14] and computer simulations [1, 6, 7]. However, as soon as latent, hidden degrees of freedom that become projected out do not relax instantaneously on the time scale we observe the reaction coordinate [15], or the reaction coordinate does not locally equilibrate in long-lived meta-stable meso-states [16], almost any projection of high-dimensional dynamics onto a lower dimensional coordinate introduces memory [15–24].

Memory effects can have intriguing manifestations in the evolution of both, ensemble- [15, 25–28] and time-average observables [15, 29], and are often particularly well-pronounced in observations that reflect, or couple to, intra-molecular distances in conformationally flexible biomolecules [16, 18, 20–22, 25, 30–38]. Moreover, if the dynamics is ergodic in the sense that the system relaxes to a unique equilibrium probability density function from any initial condition (i.e. the reaction coordinate has a unique free energy landscape) then the memory is necessarily transient [15]. Whether or not memory is in fact relevant depends on how its extent compares to the relaxation time and whether or not the latter is reached in an experiment. If the extent of memory is comparable to, or longer than, the time-scale on which biomolecules operate, such e.g. enzymes catalyzing chemical reactions [39, 40], non-Markovian effects shape biological function.

It is therefore important to assess the presence and duration of memory effects in the dynamics along reaction coordinates. An elegant “test of Markovianity” of a reaction coordinate has recently been proposed by Berezhkovskii and Makarov, who considered the behavior of transition paths [41]. The authors provide a pair of inequalities whose violation conclusively reflects that the dynamics is non-Markovian. However, memory-effects are typically transient [15] although their extent may exceed the duration of experimental observations [33]. There is thus a need to determine not only the presence

of memory in a time-series of a reaction coordinate but also its extent and attenuation at different time-scales.

Here, we fill this gap by providing a toolbox for quantifying memory in a time-series of a low-dimensional reaction coordinate. We propose a set of model-free complementary methods that are easy to use and are suited to treat reaction coordinates with arbitrary dimensionality. As a proof of concept we apply these methods to the analysis of an experimental time-series of the extension of a DNA-hairpin measured in an optical tweezers experiment and the exactly-solvable Rouse model of polymer chain.

*Theory.*— Our approach rests on a comparison of the true time-evolution with a pair reference processes: one constructed as a fictitious, Markovian time-series and the other testing for the semi-group property. Let  $q_t$  with  $0 \leq t \leq T$  denote the time-series of the reaction coordinate and  $q_t^M$  the fictitious Markovian series. Without any loss of generality we assume that the reaction coordinate is one-dimensional – the generalization to multiple dimensions is straightforward. We assume  $q_t$  and  $q_t^M$  to be ergodic with an equilibrium probability density  $p_{\text{eq}}(q)$  that is by construction identical for both processes. Let  $G(q, t|q_0) = \langle \delta(q_t - q) \rangle_{q_0}$  denote the probability density that the reaction coordinate evolving from  $q_{t=0} = q_0$  is found at time  $t$  to have a value in an infinitesimal neighborhood of  $q$  and  $G^M(q, t|q_0) = \langle \delta(q_t^M - q) \rangle_{q_0}$  the corresponding Markovian counterpart, where  $\delta(x)$  denotes Dirac’s delta function and the angular brackets  $\langle \cdot \rangle_{q_0}$  the average over all realizations of  $q_t$  evolving from  $q_0$ . We then have  $\lim_{t \rightarrow \infty} G(q, t|q_0) = \lim_{t \rightarrow \infty} G^M(q, t|q_0) = p_{\text{eq}}(q)$  as a result of ergodicity. In practice the limits are achieved as soon as  $t$  becomes sufficiently larger than the relaxation time  $t_{\text{rel}}$ , i.e.  $t \gtrsim t_{\text{rel}}$ , which may or may not be reached in an experiment. Note that the relaxation times of the true and Markovian reference process are typically not equal.

We use two descriptors, the Kullback-Leibler divergence between the transition probabilities of the true and

a fictitious reference process defined as [42]

$$\mathcal{D}_{q_0}^a(t) \equiv \int dq G(q, t|q_0) \ln[G(q, t|q_0)/G^a(q, t|q_0)], \quad (1)$$

where  $a = M, CK$  denotes the particular kind of reference process that we detail below. By construction  $\mathcal{D}_{q_0}^a(t) \neq 0$  if and only if  $G(q, t|q_0) \neq G^a(q, t|q_0)$  and thus non-zero values of  $\mathcal{D}_{q_0}^a(t)$  reflect memory in the dynamics of  $q_t$ .

When  $q_t$  reaches equilibrium in the course of the experiment we may also consider the normalized equilibrium autocorrelation function defined as

$$C_{,M}(t) \equiv \frac{\langle q_t q_0 \rangle_{,M} - \langle q \rangle_{\text{eq}}^2}{\langle q^2 \rangle_{\text{eq}} - \langle q \rangle_{\text{eq}}^2} \quad (2)$$

where we have introduced

$$\begin{aligned} \langle q_t q_0 \rangle_{,M} &\equiv \int \int q q_0 G^{,M}(q, t|q_0) p_{\text{eq}}(q_0) dq dq_0 \\ &\stackrel{T \gg t_{\text{rel}}}{\equiv} (T-t)^{-1} \int_0^{T-t} q_{\tau+t} q_\tau d\tau, \quad t \ll T, \\ \langle q^n \rangle_{\text{eq}} &\equiv \int q^n p_{\text{eq}}(q) dq, \quad \text{for } n = 1, 2 \\ &\stackrel{T \gg t_{\text{rel}}}{\equiv} T^{-1} \int_0^T q_\tau^n d\tau \end{aligned} \quad (3)$$

where the respective definitions in terms of time-averages hold if the trajectory is much longer than the relaxation time, i.e.  $T \gg t_{\text{rel}}$ . The absence of an index refers to the true process and the index  $M$  to the fictitious Markovian counterpart.

In the comparison we consider two distinct reference processes. The first one builds on the semi-group property of Markov processes, i.e. the so-called Chapman-Kolmogorov equation that we may write as

$$G_\tau^{\text{CK}}(q, t|q_0) \equiv \int G(q, t-\tau|q') G(q', \tau|q_0) dq' \quad (4)$$

because the Green's function of a time-homogeneous Markov process is time-translation invariant,  $G(q, t-\tau|q') = G(q, t|q', \tau)$  [43]. The physical interpretation of the construction is that we observe the true dynamics  $q_t$  until time  $\tau$  and then instantaneously reset the memory (if any) to zero.

If  $q_t$  is indeed memoryless we have identically  $G_\tau^{\text{CK}}(q, t|q_0) = G(q, t|q_0)$  for any  $\tau$  and thus  $\mathcal{D}_{\tau, q_0}^{\text{CK}}(t) = 0$  for any  $t$  and  $\tau$ . If  $G_\tau^{\text{CK}}(q, t|q_0) \neq G(q, t|q_0)$  for some  $t$  and  $\tau$  then  $q_t$  is conclusively non-Markovian and  $\mathcal{D}_{\tau, q_0}^{\text{CK}}(t) > 0$  but the converse is not true. Namely, there exist non-Markovian processes that satisfy the Chapman-Kolmogorov equation [15, 44]. Note that this method does not require  $q_t$  to reach equilibrium during an experiment and requires only  $G(q, t|q_0)$  that is straightforward to determine from a time series  $q_t$ . However, if equilibrium is reached then  $\lim_{t \gg t_{\text{rel}}} \mathcal{D}_{\tau, q_0}^{\text{CK}}(t) = 0$  for any  $q_0$ . By

analyzing  $\mathcal{D}_{\tau, q_0}^{\text{CK}}(t)$  we can quantify the degree of memory and its range as a function of  $\tau$  and  $q_0$  which we demonstrate below.

In the second method we construct from  $q_t$  a corresponding Markovian time-series  $q_t^M$  evolving under the influence of the potential of mean force  $w(q) \equiv -k_B T \ln p_{\text{eq}}(q)$  according to the Itô Langevin equation

$$\frac{d}{dt} q_t^M = D f(q_t^M) / k_B T + \xi_t \quad (5)$$

where  $f(q_t^M) \equiv -k_B T \partial_q \ln p_{\text{eq}}(q)|_{q=q_t^M}$  and  $\xi_t$  denotes zero mean Gaussian white noise with variance  $\langle \xi_t \xi_{t'} \rangle = 2D \delta(t-t')$  and  $D$  is the diffusion coefficient. This method assumes that we are able to determine the equilibrium probability density  $p_{\text{eq}}(q)$  and thus requires  $q_t$  to reach equilibrium. In the simplest model, which we adopt here, it is assumed that the diffusion coefficient does not depend on  $q$ . In this case inferring  $D$  is straightforward. However, we note that the best possible Markovian approximation would allow that the diffusion coefficient depends on  $q$ , i.e.  $D \rightarrow D(q)$  [45] and efficient methods have been developed to treat this case as well [46, 47]. In this case Eq. (5) is to be interpreted in the thermodynamically consistent anti-Itô or post-point convention [16].

On the level of the probability density function Eq. (5) corresponds to the Fokker-Planck equation

$$\partial_t G^M(q, t|q_0) = \partial_q D [\partial_q - (k_B T)^{-1} f(q)] G^M(q, t|q_0) \quad (6)$$

with initial condition  $G^M(q, t|q_0) = \delta(q - q_0)$  and natural boundary conditions imposed by the underlying physics. Depending on the specific problem  $G^M(q, t|q_0)$  can be found by a numerical integration of the Langevin equation and subsequent histogram analysis, i.e.  $G^M(q, t|q_0) = \langle \delta(q_t^M - q) \rangle_{q_0}$ , or directly by solving Eq. (6) as e.g. [15, 48]. In the following we illustrate both approaches.

*End-to-end distance of a Rouse polymer.* — As a first example we consider a Rouse polymer chain with  $N+1$  beads ( $N$ -bonds) in absence of hydrodynamic interactions [49, 50] and focus on the end-to-end distance as the reaction coordinate, i.e.  $q_t \equiv |\mathbf{r}_1 - \mathbf{r}_{N+1}|$ . An important feature of this model is that it is exactly solvable. We express time in units of  $t_{\text{Kuhn}}$ , the characteristic diffusion time of a Kuhn-segment, i.e.  $t_{\text{Kuhn}} = b^2/D$ , where  $b$  is the Kuhn-length and  $D$  the diffusion coefficient of a bead. The probability density function for the positions of all beads  $\{\mathbf{r}_i\}$  is well-known [49, 50] and allows us to determine exactly the probability density of the end-to-end distance. Introducing  $\nu_k \equiv k\pi/2(N+1)$ ,  $\alpha_k = 4 \sin^2(\nu_k)$  as well as  $Q_{ik} \equiv \sqrt{2/(N+1)} \cos(\nu_k[2i-1])$  and  $\eta_t \equiv \sum_{k=1}^N (Q_{1k} - Q_{Nk})^2 e^{-\alpha_k t} / 2\alpha_k$  the equilibrium probability density of  $q$  is given by  $p_{\text{eq}}(q) = q^2 e^{-q^2/4\eta_0} / 2\sqrt{\pi\eta_0}^{3/2}$  for  $q \in [0, \infty)$  with the mean extension  $\langle d \rangle = 4\sqrt{\eta_0/\pi}$

and mean square extension  $\langle d^2 \rangle = 6\eta_0$ . The probability density function of  $q$  reads exactly (for a derivation see Ref. [26])

$$G_R(q, t|q_0) = \frac{qq_0 e^{-\eta_0(q^2+q_0^2)/2(\eta_0^2-\eta_t^2)}}{p_{\text{eq}}(q)2\pi\eta_t\sqrt{\eta_0^2-\eta_t^2}} \sinh\left(\frac{\eta_t qq_0}{2(\eta_0^2-\eta_t^2)}\right). \quad (7)$$

The exact autocorrelation function in Eq. (2) is in turn obtained in the form

$$C(t) = \frac{6\sqrt{\eta_0^2-\eta_t^2}}{(3\pi-8)\eta_0} + \frac{4(\eta_0^2+\eta_t^2)\arctan\left(\eta_t/\sqrt{\eta_0^2-\eta_t^2}\right)}{(3\pi-8)\eta_0\eta_t} \quad (8)$$

The Fokker-Planck equation in the Markovian approximation to the evolution of  $q$  for the Rouse polymer (i.e. Eq. (6)) can be obtained exactly in the form of a spectral expansion [48] and reads  $G_R^M(q, t|q_0) = \sum_{k=0}^{\infty} \psi_k^R(q)\psi_k^L(q_0)e^{-kt/\eta_0}$  where

$$\psi_k^L(x) \equiv \sqrt{\frac{k!\sqrt{\pi}}{2\Gamma(3/2+k)}} L_k^{1/2}\left(\frac{x^2}{4\eta_0}\right) \quad (9)$$

where  $\Gamma(x)$  denotes the Gamma-function and  $L_k^{1/2}(x)$  the generalized Laguerre polynomial of degree  $k$  with parameter  $1/2$  (see [51]) that we compute using the Arb-library [52] and  $\psi_k^R(x) = p_{\text{eq}}(x)\psi_k^L(x)$ . Here from it is straightforward to obtain the autocorrelation function in the Markovian approximation that reads

$$C_M(t) = \frac{\sqrt{\pi}}{3-8/\pi} \sum_{k=1}^{\infty} e^{-kt/\eta_0} [k!\Gamma(3/2-k)^2\Gamma(3/2+k)]^{-1}. \quad (10)$$

A comparison of the true autocorrelation function  $C(t)$  given by Eq. (8) and the Markovian approximation  $C_M(t)$  given by Eq. (10) is shown in Fig. 1a, with the inset depicting the corresponding equilibrium probability density function  $p_{\text{eq}}(q)$ . Note that when the free energy landscape  $w(q)$  overestimates the confining effect of hidden degrees of freedom on  $q_t$  the approximate Markovian evolution always overestimates the relaxation rate (e.g. [15]; see also SM). Namely, the Markovian evolution assumes the hidden degrees of freedom to remain at equilibrium at all times whereas the instantaneous fluctuating restoring force on  $q_t$  is in this case smaller than the force arising from the free energy landscape that corresponds to the average of the fluctuating force.

The Chapman-Kolmogorov-construct for the Rouse polymer,  $G_{\tau}^{\text{CK}}(q, t|q_0)$ , is somewhat lengthy and is therefore given explicitly in the Supplementary Material, SM.  $G_{\tau}^{\text{CK}}(q, t|q_0)$  differs from Eq. (7) for all expect large values of  $t-\tau$ . A quantification of the discrepancy between the true and ‘‘Chapman-Kolmogorov’’ evolution of the end-to-end distance of the Rouse-polymer in terms of the Kullback-Leibler divergence (1) is shown in Fig. 2a.

A typical time evolution of  $\mathcal{D}_{\tau, q_0}^{\text{CK}}(t)$  gradually increases

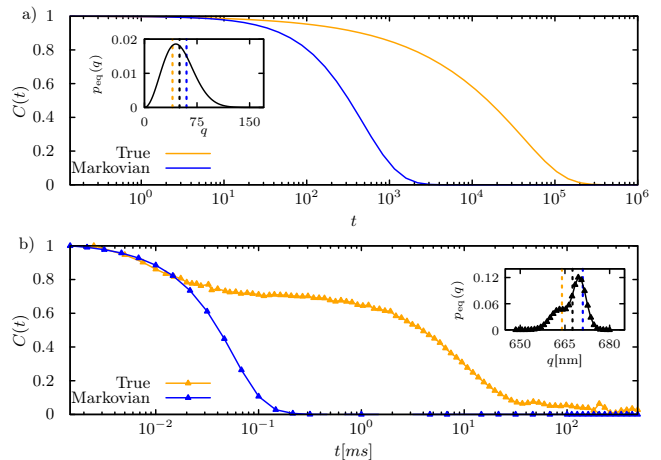


Figure 1. Comparison of the true autocorrelation function  $C(t)$  (orange) with the Markovian approximation  $C_M(t)$  (blue) for a) a Rouse-polymer with 1000 monomers with time expressed in units of the diffusion time of a Kuhn-segment  $t_{\text{Kuhn}}$ ; b) the extension of a DNA-hairpin. The insets depict the respective equilibrium probability density function  $p_{\text{eq}}(q)$ . The dashed lines depict the initial conditions we consider in Fig. 3.

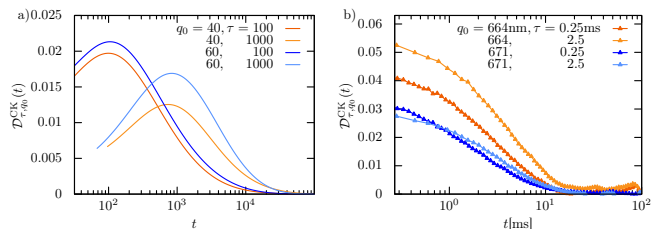


Figure 2. Kullback-Leibler divergence defined in Eq. (1) between the true Green’s function  $G(q, t|q_0)$  and the approximate Green’s function constructed from the Chapman-Kolmogorov equation (4) as a function of time  $t$  for a) the Rouse-polymer with 1000 beads and b) the extension of a DNA-hairpin. Several values of  $\tau$  are considered in the construction of  $G_{\tau}^{\text{CK}}(q, t|q_0)$  as well as a pair of different initial conditions  $q_0$ . Note that due to the particular construction of Eq. (4) times shorter than depicted are not accessible due to numerical instability and poor statistics.

from zero, reaches a maximum and afterwards returns back to 0, which reflects the gradual build-up and attenuation of memory because  $q_t$  ‘‘remembers’’ the initial condition of the hidden degrees of freedom [15]. As a result, the Chapman-Kolmogorov Green’s function  $G_{\tau}^{\text{CK}}(q, t|q_0)$  fails to predict the true evolution of  $q_t$ , and  $\mathcal{D}_{\tau, q_0}^{\text{CK}}(t)$  constructed this way depends on both,  $\tau$  and initial condition  $q_0$ . For the Rouse-polymer with 1000 beads  $\mathcal{D}_{\tau, q_0}^{\text{CK}}(t) \neq 0$  at least up to  $t \sim 10^4 \times t_{\text{Kuhn}}$ .

Next we examine  $\mathcal{D}_{q_0}^M(t)$ , the Kullback-Leibler divergence (1) between the true Green’s function  $G(q, t|q_0)$  and the Markovian approximation corresponding to the white-noise Markovian diffusion in the exact free energy

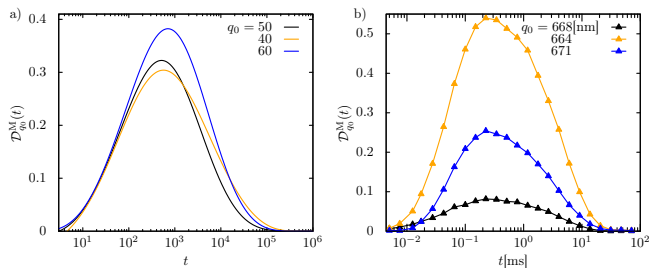


Figure 3. Kullback-Leibler divergence  $\mathcal{D}_t^M$  defined in Eq. (1) between the true Green's function  $G(q, t|q_0)$  and the Markovian approximation to the Green's function  $G^M(q, t|q_0)$  corresponding to the evolution equation (5) as a function of time  $t$  for a) the Rouse-polymer with 1000 beads evolving from  $q_0 = 40$  (orange),  $q_0 = 50$  (black),  $q_0 = 60$  (blue) and b) the extension of a DNA-hairpin evolving from a distance within a bin of thickness 1nm centered at  $q_0 = 664$  nm (orange),  $q_0 = 668$  (black) and  $q_0 = 671$  nm (blue).

landscape (i.e. Eq. (5)). The results are shown in Fig. 3a.

The qualitative features of the time-dependence of  $\mathcal{D}_{q_0}^M(t)$  are similar to those observed in Fig. 2 – memory builds up in a finite interval and smoothly returns back to zero from the attained maximum. The intuition behind this result is that it takes a finite time to allow for distinct evolutions of hidden degrees of freedom that introduce memory in the dynamics of the reaction coordinate  $q_t$ . At long times memory is progressively lost as a result of the gradual relaxation of the hidden degrees of freedom to their respective equilibrium that in turn renders the dynamics of the reaction coordinate effectively memory-less and correspondingly  $\mathcal{D}_{q_0}^M(t)$  vanishes.

*Single-molecule experiments on a DNA hairpin.* — As a second example we consider an experimental time-series of the end-to-end distance of a single-strand DNA hairpin measured in an optical tweezers experiment performed by the Woodside group [53]. The data-set contains 11 million measurements of the extension of the DNA hairpin 30R50T4 held in a pair of optical traps with stiffness 0.63 pN/nm and 1.1 pN/nm, respectively, sampled with a  $2.5\mu\text{s}$  temporal resolution. It has been shown that this time-series is non-Markovian [38]. We find the length of the time-series to be much larger than the relaxation time (see Fig. 1b) and therefore slice it into several pieces that are statistically independent. More precisely, we use a conservative estimate, namely the time-scale  $t_{\text{cut}}$  where the autocorrelation function of the extension,  $C(t)$ , falls to below  $\simeq 0.05$ . Note that this ensures  $t_{\text{cut}} \gg t_{\text{rel}}$  and yields an ensemble of 50 statistically independent trajectories.

We determine the equilibrium probability density  $p_{\text{eq}}(q)$  (see inset of Fig. 1b) and two-point joint probability density  $p(q, t, q_0, 0) = p(q, t_0 + t, q_0, t_0)$  by performing a standard histogram analysis with a bin-size

of  $l_{\text{bin}} = 0.35$  nm, such that  $q$  refers to a bin of width  $l_{\text{bin}}$  centered at  $q$ . The Greens function is thereupon obtained by the law of conditional probability,  $G(q, t|q_0) = p(q, t, q_0, 0)/p_{\text{eq}}(q)$  while the autocorrelation function in Eq. (2) is determined directly from the respective second lines of Eq. (3).

The Chapman-Kolmogorov construct is determined from  $G(q, t|q_0)$  by direct integration of Eq. (4) and is used to determine  $\mathcal{D}_{\tau, q_0}^{\text{CK}}(t)$ , while the corresponding fictitious Markovian process evolves as Markovian diffusion in a free energy landscape  $w(q) \equiv -k_B T \ln p_{\text{eq}}(q)$  with a diffusion coefficient  $D$  that we parameterize as follows. We first determine the first and second moment of the displacement from each bin-point  $q_l$  after a single time-step  $\delta t = 2.5\mu\text{s}$ , i.e.  $\langle \delta q_{\delta t}^2(l) \rangle$  and  $\langle \delta q_{\delta t}(l) \rangle$  where  $\delta q_{\delta t}(l) = q_{t+\delta t} - q_t|_{q_t=q_l}$ . We consider two bin-sizes,  $l_D = 0.01$  nm and  $l_D = 0.001$  nm, and find the result to be essentially independent on the precise value of  $l_D$  we choose (see SM). Moreover, the results are also rather independent of the location of the bin  $q_l$  (see SM), implying that to a good approximation  $D$  may indeed be taken as being constant. It is of course possible to extend the analysis to include a coordinate dependent diffusion coefficient  $D(q)$  (see e.g. [47]), which, however, is beyond the scope of this proof-of-concept paper.

From the first and second local moments of  $q$  the diffusivity  $D$  is in turn determined according to

$$D = \sum_{l=1}^{N_b} \frac{\langle \delta q_{\delta t}^2(l) \rangle - \langle \delta q_{\delta t}(l) \rangle^2}{2N_b \delta t}, \quad (11)$$

where the brackets  $\langle \cdot \rangle$  here denote the average over all displacements from this bin observed during the entire time-series. The analysis yields  $D = 447 \pm 9 \text{ nm}^2/\text{ms}$  for  $l_D = 0.001$  nm and  $D = 448 \pm 9 \text{ nm}^2/\text{ms}$  for  $l_D = 0.01$  nm, respectively. Using the values for  $D$  obtained in this way we generate the Markovian time-series  $q_t^M$  by integrating the Itô Langevin equation (5) using the Euler-Mayurama scheme, and determine  $\mathcal{D}_t^M(q_0)$  in Eq. (1) and  $C_M(t)$  in Eq. (2), respectively.

In contrast to the Rouse-polymer the DNA hairpin exists in two characteristic conformational states – folded and unfolded. As a result, the equilibrium probability density function  $p_{\text{eq}}(q)$  is bimodal and the dynamics of  $q_t$  displays signatures of metastability [53]. However, since the two peaks corresponding to the two sub-populations are not separated (see inset of Fig.1b) the potential of mean force  $w(q)$  is expected to underestimate the free energy barrier and therefore the Markovian evolution is likely to overestimate the relaxation rate. In complete agreement Fig.1b displays an overestimation of the rate of decay of autocorrelations in the Markovian approximation by two orders of magnitude in time. Moreover, a long-lived plateau is observed in the true  $C(t)$  spanning more than an order of magnitude in time.

In order to assess whether the mismatch between true and Markovian time evolution is predominantly due to an underestimation of the free energy barrier between folded and unfolded states of the hairpin we inspect the Kullback-Leibler divergence (1) between the true and “Chapman-Kolmogorov evolution” of the extension of the hairpin is shown in Fig. 2b. The result clearly shows pronounced signatures of memory in the evolution of the end-to-end distance of the hairpin that extend over more than  $\sim 10$  ms. Note that the “Chapman-Kolmogorov evolution” describes the correct evolution until time  $t = \tau$  whereupon memory is reset to zero. Therefore a non-zero  $\mathcal{D}_{\tau, q_0}^{\text{CK}}(t)$  is a clear signature of memory arising from the dynamical coupling of  $q_t$  to hidden degrees of freedom. Similar to the Rouse-polymer  $\mathcal{D}_{\tau, q_0}^{\text{CK}}(t)$  depends on the initial condition  $q_0$ .

A build-up and decay of memory similar to the Rouse-polymer is also observed in the time evolution of  $\mathcal{D}_{q_0}^{\text{M}}(t)$ , the Kullback-Leibler divergence between the Green’s function of the true evolution and the white-noise Markovian diffusion in the exact free energy landscape shown in Fig. 3b. Notably, Fig. 2b and Fig. 3b display essentially the same extent of memory (though the peak is attained sooner in the white-noise Markovian diffusion), demonstrating that metastability does not necessarily destroy nor dominate memory in the evolution of reaction coordinates. Note that the presence of memory in metastable systems is not unusual (see e.g. [20, 21] and [28]). In total, the analysis conclusively identifies the presence of extended memory effects in the dynamics of the extension of the hairpin.

It is important to note that the extent of memory (of the order of  $\sim 10$ ms) is clearly shorter than the relaxation time (compare Figs. 1b and 3b), and therefore the decay of memory does not coincide with the relaxation time and the corresponding “forgetting” of initial conditions of the coordinate itself. Instead the memory reflects the correlations between  $q_t$  and the initial conditions of the hidden degrees of freedom [15]. The information encoded in  $C(t)$  and  $\mathcal{D}^{\text{M,CK}}(t)$  is therefore different –  $\mathcal{D}^{\text{M,CK}}(t)$  is a genuine measure of the extent and duration of memory.

*Conclusion.*— We presented a set of complementary methods to quantify conclusively the degree and duration of memory in a time series of a reaction coordinate  $q_t$ . The proposed toolbox does not assume any particular physical model. Instead it exploits the semi-group property of Markov processes and constructs a fictitious Markovian diffusion process in the free energy landscape of  $q_t$ , and compares the artificially constructed transition probability density with the observed probability density. The analysis not only determines whether the dynamics of  $q_t$  has memory but also quantifies the magnitude and duration of memory and thus complements the recently proposed “test for Markovianity” based on transition paths [41]. Whereas in our examples we considered only one-dimensional coordinates and constant

diffusion coefficients the toolbox generalizes straightforwardly to higher-dimensional reaction coordinates and diffusion landscapes  $D(q)$ . The method is general, robust, and easy to use. We therefore hope that it will find numerous applications involving time-series derived from experiments and computer simulations.

*Acknowledgments* We thank Krishna Neupane and Michael T. Woodside for providing unlimited access to their DNA-hairpin data. The financial support from the German Research Foundation (DFG) through the Emmy Noether Program GO 2762/1-1 to AG is gratefully acknowledged.

---

\* agodec@mpibpc.mpg.de

- [1] R. B. Best and G. Hummer, Reaction coordinates and rates from transition paths, *Proc. Natl. Acad. Sci.* **102**, 6732–6737 (2005).
- [2] J. J. Portman, S. Takada, and P. G. Wolynes, Microscopic theory of protein folding rates. ii. local reaction coordinates and chain dynamics, *J. Chem. Phys.* **114**, 5082–5096 (2001).
- [3] B. Peters, P. G. Bolhuis, R. G. Mullen, and J.-E. Shea, Reaction coordinates, one-dimensional smoluchowski equations, and a test for dynamical self-consistency, *J. Chem. Phys.* **138**, 054106 (2013).
- [4] A. K. Faradjian and R. Elber, Computing time scales from reaction coordinates by milestoning, *J. Chem. Phys.* **120**, 10880–10889 (2004).
- [5] A. Berezhkovskii and A. Szabo, One-dimensional reaction coordinates for diffusive activated rate processes in many dimensions, *J. Chem. Phys.* **122**, 014503 (2005).
- [6] G. Hummer, Position-dependent diffusion coefficients and free energies from bayesian analysis of equilibrium and replica molecular dynamics simulations, *New J. Phys.* **7**, 34–34 (2005).
- [7] R. B. Best and G. Hummer, Coordinate-dependent diffusion in protein folding, *Proc. Natl. Acad. Sci.* **107**, 1088–1093 (2009).
- [8] W. Zhang, C. Hartmann, and C. Schütte, Effective dynamics along given reaction coordinates, and reaction rate theory, *Faraday Discussions* **195**, 365–394 (2016).
- [9] A. M. Berezhkovskii and D. E. Makarov, Communication: Coordinate-dependent diffusivity from single molecule trajectories, *J. Chem. Phys.* **147**, 201102 (2017).
- [10] O. K. Dudko, G. Hummer, and A. Szabo, Theory, analysis, and interpretation of single-molecule force spectroscopy experiments, *Proceedings of the National Academy of Sciences* **105**, 15755–15760 (2008).
- [11] K. Neupane, A. P. Manuel, and M. T. Woodside, Protein folding trajectories can be described quantitatively by one-dimensional diffusion over measured energy landscapes, *Nat. Phys.* **12**, 700 (2016).
- [12] K. Neupane, D. A. N. Foster, D. R. Dee, H. Yu, F. Wang, and M. T. Woodside, Direct observation of transition paths during the folding of proteins and nucleic acids, *Science* **352**, 239 (2016).
- [13] J. Gladrow, M. Ribezzi-Crivellari, F. Ritort, and U. F. Keyser, Experimental evidence of symmetry breaking of transition-path times, *Nat. Commun.* **10**, 10.1038/s41467-

- 018-07873-9 (2019).
- [14] A. L. Thorneywork, J. Gladrow, Y. Qing, M. Rico-Pasto, F. Ritort, H. Bayley, A. B. Kolomeisky, and U. F. Keyser, Direct detection of molecular intermediates from first-passage times, *Sci. Adv.* **6**, 10.1126/sciadv.aaz4642 (2020).
- [15] A. Lapolla and A. Godec, Manifestations of Projection-Induced Memory: General Theory and the Tilted Single File, *Front. Phys.* **7**, 10.3389/fphy.2019.00182 (2019).
- [16] D. Hartich and A. Godec, Emergent memory and kinetic hysteresis in strongly driven networks, arXiv:2011.04628 (2020), arXiv:2011.04628 [cond-mat.stat-mech].
- [17] N. van Kampen, Remarks on Non-Markov Processes, *Brazilian J. Phys.* **28**, 10.1590/S0103-97331998000200003 (1998).
- [18] S. S. Plotkin and P. G. Wolynes, Non-markovian configurational diffusion and reaction coordinates for protein folding, *Phys. Rev. Lett.* **80**, 5015 (1998).
- [19] R. Zwanzig, *Nonequilibrium statistical mechanics* (Oxford Univ. Press, 2010).
- [20] D. E. Makarov, Interplay of non-markov and internal friction effects in the barrier crossing kinetics of biopolymers: Insights from an analytically solvable model, *J. Chem. Phys.* **138**, 014102 (2013).
- [21] M. Ozmaian and D. E. Makarov, Transition path dynamics in the binding of intrinsically disordered proteins: A simulation study, *J. Chem. Phys.* **151**, 235101 (2019).
- [22] H. Meyer, P. Pelagejcev, and T. Schilling, Non-markovian out-of-equilibrium dynamics: A general numerical procedure to construct time-dependent memory kernels for coarse-grained observables, *EPL (Europhys. Lett.)* **128**, 40001 (2020).
- [23] E. Herrera-Delgado, J. Briscoe, and P. Sollich, Tractable nonlinear memory functions as a tool to capture and explain dynamical behaviors, *Phys. Rev. Research* **2**, 043069 (2020).
- [24] F. Müller, U. Basu, P. Sollich, and M. Krüger, Coarse-grained second-order response theory, *Phys. Rev. Research* **2**, 043123 (2020).
- [25] W. Min, G. Luo, B. J. Cherayil, S. C. Kou, and X. S. Xie, Observation of a power-law memory kernel for fluctuations within a single protein molecule, *Phys. Rev. Lett.* **94**, 198302 (2005).
- [26] A. Lapolla and A. Godec, Faster uphill relaxation in thermodynamically equidistant temperature quenches, *Phys. Rev. Lett.* **125**, 10.1103/physrevlett.125.110602 (2020).
- [27] A. Lapolla and A. Godec, Bethesf: Efficient computation of the exact tagged-particle propagator in single-file systems via the bethe eigenspectrum, *Comput. Phys. Commun.* **258**, 107569 (2021).
- [28] A. Lapolla and A. Godec, Single-file diffusion in a bistable potential: Signatures of memory in the barrier-crossing of a tagged-particle, *J. Chem. Phys.* **153**, 194104 (2020).
- [29] A. Lapolla and A. Godec, Unfolding tagged particle histories in single-file diffusion: exact single- and two-tag local times beyond large deviation theory, *New J. Phys.* **20**, 113021 (2018).
- [30] S. C. Kou and X. S. Xie, Generalized langevin equation with fractional gaussian noise: Subdiffusion within a single protein molecule, *Phys. Rev. Lett.* **93**, 180603 (2004).
- [31] T. Neusius, I. Daidone, I. M. Sokolov, and J. C. Smith, Subdiffusion in peptides originates from the fractal-like structure of configuration space, *Phys. Rev. Lett.* **100**, 188103 (2008).
- [32] S. Pressé, J. Peterson, J. Lee, P. Elms, J. L. MacCallum, S. Marqusee, C. Bustamante, and K. Dill, Single molecule conformational memory extraction: P5ab rna hairpin, *J. Phys. Chem. B* **118**, 6597–6603 (2014).
- [33] X. Hu, L. Hong, M. Dean Smith, T. Neusius, X. Cheng, and J. Smith, The dynamics of single protein molecules is non-equilibrium and self-similar over thirteen decades in time, *Nature Physics* **12**, 171–174 (2015).
- [34] A. K. Sangha and T. Keyes, Proteins Fold by Subdiffusion of the Order Parameter, *J. Phys. Chem. B* **113**, 15886 (2009).
- [35] S. M. Avdoshenko, A. Das, R. Satija, G. A. Papoian, and D. E. Makarov, Theoretical and computational validation of the Kuhn barrier friction mechanism in unfolded proteins, *Sci. Rep.* **7**, 269 (2017).
- [36] Y. Cote, P. Senet, P. Delarue, G. G. Maisuradze, and H. A. Scheraga, Anomalous diffusion and dynamical correlation between the side chains and the main chain of proteins in their native state, *Proc. Natl. Acad. Sci.* **109**, 10346 (2012).
- [37] I. Grossman-Haham, G. Rosenblum, T. Namani, and H. Hofmann, Slow domain reconfiguration causes power-law kinetics in a two-state enzyme, *Proc. Natl. Acad. Sci.* **115**, 513 (2018).
- [38] A. G. T. Pyo and M. T. Woodside, Memory effects in single-molecule force spectroscopy measurements of biomolecular folding, *Phys. Chem. Chem. Phys.* **21**, 24527 (2019).
- [39] H. P. Lu, Single-molecule enzymatic dynamics, *Science* **282**, 1877–1882 (1998).
- [40] B. P. English, W. Min, A. M. van Oijen, K. T. Lee, G. Luo, H. Sun, B. J. Cherayil, S. C. Kou, and X. S. Xie, Ever-fluctuating single enzyme molecules: Michaelis-menten equation revisited, *Nat. Chem. Biol.* **2**, 87–94 (2005).
- [41] A. M. Berezhkovskii and D. E. Makarov, Single-Molecule Test for Markovianity of the Dynamics along a Reaction Coordinate, *J. Phys. Chem. Lett.* **9**, 2190 (2018).
- [42] S. Kullback and R. Leibler, On information and sufficiency, *Ann. Math. Statist* **22**, 79 (1951).
- [43] Gardiner, C.W., *Handbook of Stochastic Methods for Physics, Chemistry and Natural Sciences*, 2nd ed. (Springer-Verlag, 1985).
- [44] W. Feller, Non-Markovian Processes with the Semigroup Property, *The Annals of Mathematical Statistics* **30**, 1252 (1959).
- [45] A. Berezhkovskii and A. Szabo, Time scale separation leads to position-dependent diffusion along a slow coordinate, *J. Chem. Phys.* **135**, 074108 (2011).
- [46] B. J. Berne, M. Borkovec, and J. E. Straub, Classical and modern methods in reaction rate theory, *J. Phys. Chem.* **92**, 3711–3725 (1988).
- [47] G. Hummer, Position-dependent diffusion coefficients and free energies from bayesian analysis of equilibrium and replica molecular dynamics simulations, *New J. Phys.* **7**, 34 (2005).
- [48] S. Sunagawa and M. Doi, Theory of Diffusion-Controlled Intrachain Reactions of Polymers, *Polymer J.* **7**, 604 (1975).
- [49] P. E. Rouse, A Theory of the Linear Viscoelastic Properties of Dilute Solutions of Coiling Polymers, *J. Chem. Phys.* **21**, 1272 (1953).
- [50] K. H. Ahn, J. L. Schrag, and S. J. Lee, Bead-spring chain model for the dynamics of dilute polymer solutions, *J.*

- Non-Newton Fluid Mech. **50**, 349 (1993).
- [51] Abramowitz, Milton and Stegun, Irene A., Handbook of Mathematical Functions with Formulas, Graphs, and Mathematical Tables, in *Handbook of Mathematical Functions with Formulas, Graphs, and Mathematical Tables* (Dover, New York, 1964) ninth dover printing, tenth printing ed.
- [52] F. Johansson, Arb: Efficient Arbitrary-Precision Midpoint-Radius Interval Arithmetic, IEEE Transactions on Computers **66**, 1281 (2017).
- [53] K. Neupane, A. P. Manuel, J. Lambert, and M. T. Woodside, Transition-Path Probability as a Test of Reaction-Coordinate Quality Reveals DNA Hairpin Folding Is a One-Dimensional Diffusive Process, J. Phys. Chem. Lett. **6**, 1005 (2015).

**Supplementary Material for:  
A Toolbox for Quantifying Memory in Dynamics Along Reaction Coordinates**

Alessio Lapolla and Aljaž Godec

*Mathematical bioPhysics Group, Max Planck Institute for Biophysical Chemistry, 37077 Göttingen, Germany*

**Abstract**

In this Supplementary Material (SM) we present the exact result for the ‘‘Champman-Kolmogorov’’ construction of the Green’s function of the end-to-end distance and other internal coordinates of the Rouse polymer defined in Eq. (4) in the manuscript as well as a local error analysis of the inferred diffusion coefficient  $D$  entering the Markovian approximation of the end-to-end diffusion of the DNA hairpin. In addition, supplementary figures are included showing the various Green’s functions for the Rouse polymer and DNA hairpin.

**DETAILS OF THE PROJECTION AFFECT THE RELAXATION TIME AND EXTENT OF MEMORY**

In the main text we consider Rouse polymer chain composed of 1000 beads and we focus on the autocorrelation function of its end-to-end distance as the reaction coordinate  $q_t$ . We find that the fictitious Markovian reference process describing Brownian diffusion in the free energy landscape overestimates the relaxation rate; a similar observation is also made in the case of the experimental hairpin data. However this difference in the rate of relaxation is non-unique and in fact depends on the observable, i.e. on details of the projection.

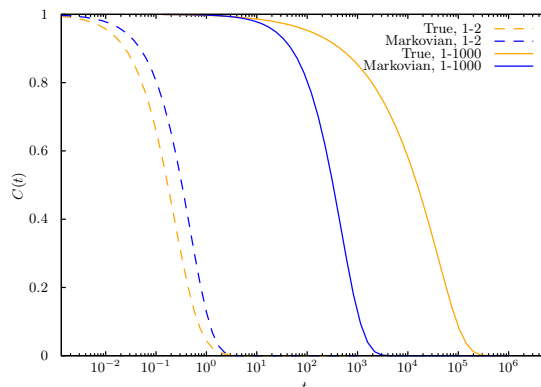


Figure S4. The autocorrelation function of the distance between the first and the second bead (dashed lines) and first and last bead (full lines) of a Rouse chain composed by 1000 according to the true (orange) and fictitious Markovian evolution (blue). Note the the free energy landscape for both orange-blue pairs is by construction identical. The continuous lines are those shown in the main text.

For example we demonstrate in Fig. S4 the opposite trend that arises when we observe the autocorrelation function of the distance between the first and the second bead of the same Rouse Chain (see dashed lines).

In addition, is worth to note that if the Green’s function  $\mathcal{G}$  describing the full many-dimensional system is diagonalizable (like in the Rouse chain case [1] or any Markovian dynamics obeying detailed balance), it can be written as

$$\mathcal{G}(\mathbf{x}, t|\mathbf{x}_0) = \sum_k \psi_k^R(\mathbf{x})\psi_k^L(\mathbf{x}_0)e^{-\lambda_k t}, \quad (\text{S1})$$

where  $\psi_k^R$  and  $\psi_k^L$  are respectively the right and left eigenfunctions of the underlying Fokker-Planck-Smoluchowski operator, while  $\lambda_k$  denotes the eigenvalues. Then the Green’s function of the projected observable – the reaction coordinate  $q = \Gamma(\mathbf{x})$  – can be written in full generality [2] as

$$G(q, t|q_0) = \sum_k V_k^R(q; \Gamma)V_k^L(q_0; \Gamma)e^{-\lambda_k t}, \quad (\text{S2})$$

where the elements  $V_k^R$  and  $V_k^L$  depend both on  $\psi_k^R$  and  $\psi_k^L$ , and on the projection  $\Gamma(\mathbf{x})$ . In turn the autocorrelation function can be easily computed as:

$$C(t) = \sum_k \left( \int q V_k^R(q; \Gamma) dq \right) \left( \int q_0 V_k^L(q_0; \Gamma) dq_0 \right) e^{-\lambda_k t} \equiv \sum_k a_k^{R, \Gamma} b_k^{L, \Gamma} e^{-\lambda_k t}, \quad (\text{S3})$$

and one can show that for systems obeying detailed balance  $a_k^{R, \Pi} b_k^{L, \Pi} \geq 0$  [2]. The analysis shows that the projection only affects the weights whereas the exponentiated eigenvalues (and thus time-scales) are those of the full system's dynamics.

Nevertheless, the autocorrelation function of different observables of the same system may decay on widely disparate time-scales; compare the dashed and continuous lines in Fig. S4 where in the end-to-end distance the relaxation time is  $\sim 10^6$  while in the first-to-second distance is  $\sim 10^1$ . This disparity is simply a result of the projection that determines the relative contribution of different eigenfunctions.

### THE CHAPMAN-KOLMOGOROV CONSTRUCTION

In the case of the Rouse chain the integral defined in Eq. (4) in the main text can be solved analytically via a straightforward but tedious calculation using Eq. (7) in the main text. The result of the integral reads exactly

$$G_{t_1}^{CK}(q, t|q_0) = \frac{\eta_0^{7/2} q}{q_0 \eta_{t-\tau} \eta_\tau \sqrt{\pi \Xi_{\tau, t-\tau}}} \sinh \left( \frac{qq_0 \eta_0 \eta_\tau \eta_{t-\tau}}{2 \Xi_{\tau, t-\tau}} \right) \times \exp \left[ -\frac{q^2 \eta_0}{2 \Omega_{t-\tau}^-} \left( 1 - \frac{\eta_{t-\tau}^2 \Omega_\tau^-}{2 \Xi_{\tau, t-\tau}} \right) - \frac{q_0^2}{4 \Omega_\tau^-} \left( \frac{\eta_0^2 \Omega_\tau^- - \eta_{t-\tau}^2 \Omega_\tau^+}{\Omega_{t-\tau}^-} - \frac{\eta_0 \eta_\tau^2 \Omega_{t-\tau}^-}{\Xi_{\tau, t-\tau}} \right) \right] \quad (\text{S4})$$

having defined

$$\Omega_t^\pm = \eta_0^2 \pm \eta_t^2, \quad \Xi_{\tau, t-\tau} = 4\eta_0^4 - \Omega_\tau^+ \Omega_{t-\tau}^+. \quad (\text{S5})$$

Notably, the structure of Eq. (S4) is identical to the structure of the plain Green's function (Eq. (7) in the main text) but here the temporal dependence is obviously different.

Note that in when the observation time is much larger than the relaxation time of the observable  $t_{\text{rel}}$ , we find for  $t - \tau > t_{\text{rel}}$  that  $G_\tau^{\text{CK}}(q, t|q_0) \simeq p_{\text{eq}}(q) \int dq' G(q', t|q_0) = p_{\text{eq}}(q)$ . Therefore, since  $\lim_{t \rightarrow \infty} G(q, t|q') = p_{\text{eq}}(q)$ , the definition of  $G_\tau^{\text{CK}}(q, t|q_0)$  (Eq. (4) in the main text) by construction ensures  $\lim_{t \rightarrow \infty} \mathcal{D}_{\tau, q_0}^{\text{CK}}(t) = 0$ . In Fig. S5 we explicitly show the Green's function that is required for the computation of the Kullback-Liebler divergence.

### ESTIMATION OF THE DIFFUSION COEFFICIENT

Eq. (12) in the main text demonstrates how one can estimate the ( $q$ -independent) diffusion coefficient  $D$  from a time-series using the first two moments of the local displacement.

The moments are in turn determined as follows: if  $q_t$  is found during an epoch in the bin centered around  $q$  and of size  $l_D$  its displacement from the previous epoch is determined and its square and both are averaged over all epochs in the time-series yielding  $\langle \delta q_{\delta t} \rangle$  and  $\langle \delta q_{\delta t}^2 \rangle$  respectively.

This procedure is repeated for different positions  $q$  on the support of the equilibrium distribution. We find that the resulting diffusion coefficient changes little over the entire support even for different bin-sizes  $l_D$  (see Fig. S6). Therefore we treat it, as a first approximation, as being independent of  $q$  and average over all bins to obtain  $D \simeq \overline{D} = 448 \text{ nm}^2/\text{ms}$ . Using this value of  $D$  we perform Brownian Dynamics simulations of the fictitious Markovian process according to the Euler-Mayurama scheme.

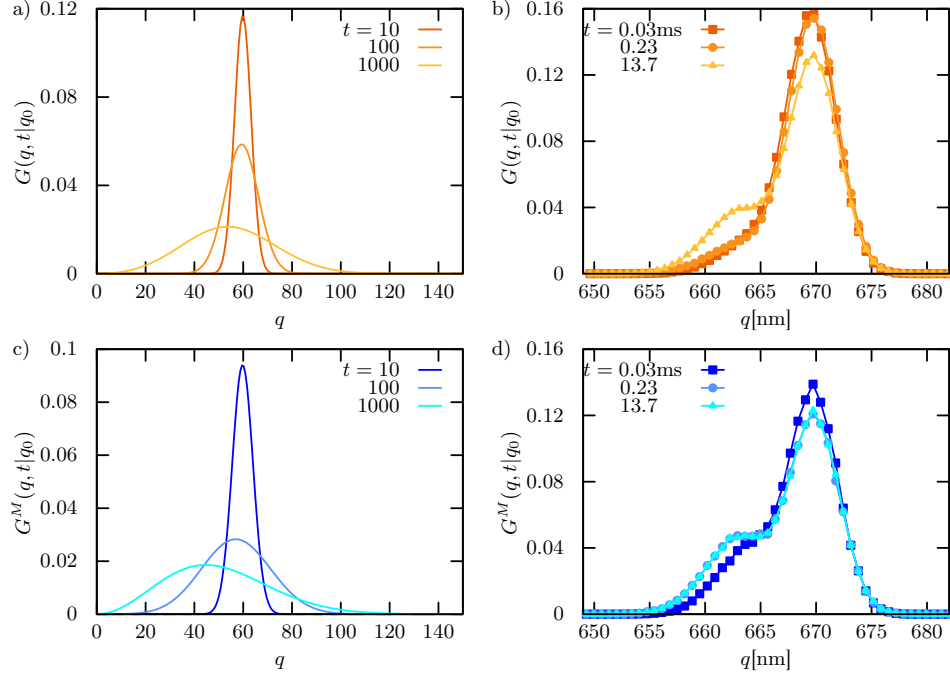


Figure S5. Green's function at different times for both considered systems. a) and b) depict the true Green's function for the end-to-end distance of the Rouse chain and of the DNA hairpin respectively. Panels c) and d) show the Green's function of their respective fictitious Markovian processes at the same times. The initial conditions are  $q_0 = 60$  for the Rouse chain and  $q_0 = 671$  nm for the hairpin.

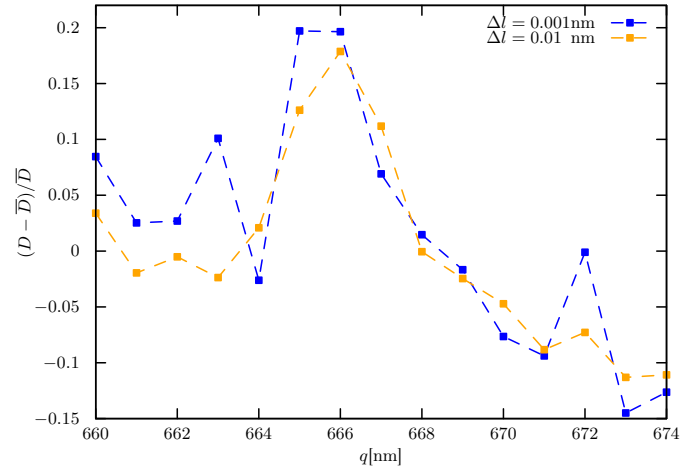


Figure S6. Relative deviation of the local diffusion coefficient in a given bin  $D_l$  from the average value  $\bar{D} = N^{-1} \sum_{l=1}^N D_l$  as a function of the position of the bin. In the case of  $\Delta l = 0.001$  nm we find  $\bar{D} = 447$  nm<sup>2</sup>/ms with a deviation  $\pm 9$  nm<sup>2</sup>/ms and for  $\Delta l = 0.01$  nm we find  $\bar{D} = 448$  nm<sup>2</sup>/ms with a deviation  $\pm 9$  nm<sup>2</sup>/ms. In a first approximation the values of  $D_l$  are independent of  $l$  and we thus set  $D \approx \bar{D} \simeq 448$  nm<sup>2</sup>/ms.

---

\* agodec@mpibpc.mpg.de

- [1] G. Wilemski and M. Fixman, Diffusion-controlled intrachain reactions of polymers. I Theory, *J. Chem. Phys.* **60**, 866 (1974).
- [2] A. Lapolla and A. Godec, Manifestations of Projection-Induced Memory: General Theory and the Tilted Single File, *Front. Phys.* **7**, 10.3389/fphy.2019.00182 (2019).